Original Article

Utilizing network pharmacology and experimental validation to explore the potential molecular mechanisms of raw *Pinellia ternate* in treating esophageal cancer

Yanxin Liu[1], Yunfei Bai[1], Jinbang Zhang[1], Reginaldo Silva-Filho[2], Qingchun Zhu[1], Zhen Lei[3]

[1]Department of Pharmacy, Henan Provincial Hospital of Traditional Chinese Medicine (The Second Affiliated Hospital of Henan University of Traditional Chinese Medicine), Zhengzhou, China; [2]Faculdade EBRAMEC, São Paulo, Brazil; [3]Central Laboratory, Henan Provincial Hospital of Traditional Chinese Medicine (The Second Affiliated Hospital of Henan University of Traditional Chinese Medicine), Zhengzhou, China

Contributions: (I) Conception and design: Y Liu; (II) Administrative support: Y Bai; (III) Provision of study materials or patients: Y Liu, Y Bai; (IV) Collection and assembly of data: J Zhang, Q Zhu; (V) Data analysis and interpretation: Y Bai, J Zhang, Z Lei; (VI) Manuscript writing: All authors; (VII) Final approval of manuscript: All authors.

Correspondence to: Yanxin Liu, BS. Department of Pharmacy, Henan Provincial Hospital of Traditional Chinese Medicine (The Second Affiliated Hospital of Henan University of Traditional Chinese Medicine), No. 6 Dongfeng Road, Jinshui District, Zhengzhou 450053, China. Email: hzylw@hactcm.edu.cn.

Background: Esophageal cancer (EC) is a highly lethal malignancy with a grim prognosis and high mortality rates, primarily treated through surgery and radiotherapy. Herbal remedies are emerging as complementary approaches in cancer therapy. Here, we explore the potential therapeutic benefits of Chinese medicine raw *Pinellia ternata* (RP) in EC using web-based pharmacological methods and cellular experiments.

Methods: The chemical components of RP were obtained by data mining via searches of the systematic pharmacology database, analysis platform, and literature on traditional Chinese medicine (TCM). The properties of the main components of RP were calculated using Traditional Chinese Medicine Systems Pharmacology Database and Analysis Platform (TCMSP). The potential targets of the components were mined and collected through multiple databases, and the relevant potential targets of efficacy were imported into Search Tool for the Retrieval of Interacting Genes/Proteins (STRING) database to obtain protein interactions. Gene Ontology (GO) enrichment analysis and Kyoto Encyclopedia of Genes and Genomes (KEGG) metabolic pathway enrichment analysis of the potential targets were performed through Metascape. A target-pathway network was established using Cytoscape, and topological analysis was performed on the network so as to obtain the relevant targets and pathways of RP in the treatment of EC. The inhibitory effect of RP on human EC cells was verified by cell experiments.

Results: Thirteen bioactive components of RP were screened, 87 related targets were obtained by construction, and 68 co-targets were obtained after taking intersection with EC related genes. The results of the protein-protein interaction (PPI) network analysis of the targets showed that the pharmacodynamic targets of hemicellulose might be closely related to the signaling pathways such as PI3K-Akt, FOS/JUN, and HIF-1. Meanwhile, GO and KEGG enrichment analysis showed that PI3K-Akt was also significantly enriched. The *in vitro* cellular experiments further indicated that raw hemicrania could inhibit EC through the PI3K-Akt signaling pathway.

Conclusions: The pharmacodynamic mechanism of RP in the treatment of esophageal carcinoma was preliminarily revealed, which provided ideas and the basis for further experimental study of RP in the treatment of esophageal carcinoma.

Keywords: Raw *Pinellia ternata* (RP); esophageal cancer (EC); network pharmacology; PI3K-Akt signal pathway

Submitted Aug 15, 2023. Accepted for publication Oct 20, 2023. Published online Oct 27, 2023.
doi: 10.21037/jgo-23-684
View this article at: https://dx.doi.org/10.21037/jgo-23-684

Introduction

Esophageal cancer (EC) is a prevalent malignancy in China, with high morbidity and mortality rates (1). Modern medicine offers several therapeutic schemes for EC, including surgical resection, chemotherapy, radiotherapy, and combined therapy. Although EC treatment and diagnostic techniques continue to evolve, because most patients are found at an advanced stage and are inoperable or have metastatic disease, the 5-year survival rate is only 15–25%, and for metastatic EC, the 5-year survival rate is only 4%, with the prognosis being very poor (2,3). At present, the application of targeted agents in EC is quite restricted, with only human epidermal growth factor receptor 2 (HER2) or vascular endothelial growth factor (VEGF) targeted therapies available for esophageal adenocarcinoma (EAC). On the other hand, immunotherapy has shown promising advancements in overall and progression-free survival, but its effectiveness is observed only in a specific group of patients who were not pre-screened and treated with immunotherapeutics. It is therefore critical to explore new therapeutic drugs that offer high specificity, good curative effects, and low toxicity and side effects in the development of anticancer drugs. In a review of the prescription records of patients with EC admitted to the Department of Oncology of the Second Affiliated Hospital of Henan University of Traditional Chinese Medicine in the past 5 years, it was found that more than 90% of these patients were administered traditional Chinese medicine (TCM) decoction adjuvant in chemotherapy; further analysis of each prescription revealed that raw *Pinellia ternata* (RP) had a particularly prominent role in each prescription.

RP is the dried tuber of *Pinellia ternata* (*Thunb.*) *Makino*, known as Ban Xia in Chinese medicine, a member of the *Araceae* family and has the effects of removing dampness and phlegm, reducing adverse effects and stopping vomiting, eliminating phlegm and dispersing mass, reducing swelling, and relieving pain (4). It is generally accepted that its tubers are toxic, and *Pinellia ternata* (*P. ternata*) is generally used as a medicine after processing to reduce the occurrence of its adverse reactions. However, modern pharmacological studies have found that RP contains a variety of chemical components, such as alkaloids, organic acids, amino acids, volatile oils, flavonoids, *P. ternata* starch, sterols, aromatic components, *P. ternata* protein, sugars, and a variety of trace elements, and has anti-inflammatory, antitumor, and antibacterial pharmacological effects (5,6). *P. ternata* is the main clinical treatment for a variety of malignant tumors. In this study, the pharmacodynamic mechanism of RP in the treatment of EC was explored by network pharmacology technology and verified in combination with cell experiments in order to reveal the material basis of RP in the treatment of EC and the possible pathway mechanism of the pharmacodynamic action. We present this article in accordance with the MDAR reporting checklist (available at https://jgo.amegroups.com/article/view/10.21037/jgo-23-684/rc).

Highlight box

Key findings

- Raw *Pinellia ternata* inhibits the migration and invasion of esophageal cancer cells via the PI3K-Akt signaling pathway.

What is known and what is new?

- In clinical treatment, raw *Pinellia ternata* is used to treat a variety of malignant tumors, including esophageal cancer. Meanwhile, the PI3K-Akt signaling pathway is closely related to the development of many human tumors.
- The main active ingredient type and the main target of raw *Pinellia ternata* in esophageal cancer is Akt. And *in vitro* experiments have shown that raw *Pinellia ternata* prevents esophageal cancer progression by inhibiting the PI3K-Akt signaling pathway.

What is the implication, and what should change now?

- The bioactive active ingredient of raw *Pinellia ternata* that exerts an antinodal esophageal cancer effect was identified, and the molecular mechanism of antagonism is the inhibition of the PI3K-Akt signaling pathway. We can subsequently verify other pathways of raw *Pinellia ternata* for the treatment of esophageal cancer.

Methods

Network pharmacological analysis

Establishment of chemical composition database and target prediction

All chemical constituents of RP were first searched from the Traditional Chinese Medicine Systems Pharmacology Database and Analysis Platform (TCMSP, https://old.tcmsp-e.com/tcmsp.php) and PubChem databases (https://pubchem.ncbi.nlm.nih.gov/) to establish a database of chemical constituents of *P. ternata*. Oral bioavailability (OB) ≥30% and drug-like (DL) ≥0.18 (7) were screened and collated to obtain the active components of RP drugs; the TCMSP data platform was used to obtain the corresponding target proteins according to the active components and to delete duplicates; the target proteins corresponding to each active component were converted to the corresponding gene names for further mechanistic

studies. The UniProt database (https://www.uniprot.org/uniprotkb) was used to standardize the names of targets of action for chemical constituents.

EC-related target prediction

Using "esophageal cancer" as the keyword, we searched the GeneCards (https://www.genecards.org), Therapeutic Target Database (TTD 4.3.02, https://db.idrblab.net/ttd/), Drugbank 3.0 (https://www.drugbank.ca/), and DisGeNET (https://www.disgenet.org/) databases to obtain EC-related disease targets and remove duplicate targets. In order to obtain targets more relevant to EC, median values were filtered according to the score, and targets were normalized using the UniProt database.

Gene Ontology (GO) and Kyoto Encyclopedia of Genes and Genomes (KEGG) enrichment analysis

Venny 2.1 software was used to draw Wayne plots to find cross-targets. GO enrichment analysis and KEGG signaling pathway enrichment analysis was performed using the Metascape platform (https://metascape.org/), a biological information annotation database. The target genes were imported into this database, with $P<0.01$ and enrichment ≥ 1.5 being used as the significance threshold to predict the GO pathway involved in the target of the main active component of *P. ternata*. Similarly, $P<0.01$ and enrichment ≥ 1.5 conditions were used as KEGG pathway enrichment analysis thresholds to predict the signaling pathways targeted by the main active component targets of *P. ternata*.

Construction of a compound-component-target-pathway network

On the basis of pathway enrichment analysis, Cytoscape 3.6.1 software was used to construct the network relationship diagram of RP component-target-pathway-EC according to the important signaling pathways and their corresponding targets and the main active components of RP. A protein-protein interaction (PPI) network model of the common target for raw hemimelia EC was constructed by Search Tool for the Retrieval of Interacting Genes/Proteins (STRING, https://string-db.org/) online platform and embellished with Cytoscape 3.6.1 software through Degree (BC) parameter.

Cell experiments

Cell culture

EC Eca-109 cells were purchased from the Cell Bank of Shanghai Chinese Academy of Sciences and cultured in Dulbecco's Modified Eagle Medium (DMEM) medium containing 10% fetal bovine serum (FBS), 1% penicillin, and 1% streptomycin. Cells were incubated in a 5% CO_2 incubator at 37 ℃.

Cell Counting Kit 8 (CCK-8) cell viability assay

Eca-109 cells in the logarithmic growth phase were seeded into 96-well plates at 100 μL per well, and the cell density was adjusted to 2×10^4 cells per milliliter. Different concentrations of RP (0, 0.025, 0.05, 0.1, 0.2, 0.4, 0.8 mg/mL) were added to each well and cultured in an incubator at 5% CO_2 and 37 ℃ for 24 h. CCK-8 solution was added to each well at a concentration of 10 μL and incubated at 37 ℃ for 2 h. Absorbance values at 490 nm were measured with an enzyme calibration meter.

Preparation of RP extract

RP originating from mainland China was purchased from Henan Chinese herbal medicine market. Dried 500 g of RP was ground into coarse powder, decocted with 10 times the amount of water for 2 times, 2 hours each time, filtered and combined the filtrate, evaporated, and then the remaining aqueous extract was freeze-dried.

Scratch assay for cell migration

Eca-109 cells in logarithmic growth phase were inoculated into 6-well plates, at about 5×10^5 cells per well, and divided into a control group (saline), tumor necrosis factor alpha (TNF-α) group, and RP group. On day 2, when cells grew to 100% confluence, a straight line with consistent force and angle and uniform thickness was drawn gently at the bottom of a 6-well plate with a sterile 10-μL tip (3 replicates for each group). The width of scratches in the same field was observed and photographed under an inverted phase contrast microscope at 0 and 24 h. The scratch healing distance was calculated as follows: distance (μm) = scratch width at 0 h – scratch width at 24 h. The scratch healing distance was used to represent the cell migration ability.

Transwell chamber assay for cell invasion

Matrigel was precooled at 4 ℃, diluted in a 1:5 ratio, added to the upper chamber of the Transwell, spread well, and dried at 37 ℃ for 70 min. The groups were the same as those described for the scratch assay. Five replicate wells were set up in each group to adjust the cell concentration to 5×10^5 cells per milliliter, 200 μL cell suspension was added upwards, and 500 μL of medium containing 20% FBS was added downwards as a chemokine. After the addition of the

Table 1 Major active compounds of *Pinellia ternata*

TCMSP No.	Compound	Bioavailability (%)	Drug-like	No. of targets
MOL001755	24-Ethylcholest-4-en-3-one	36.08	0.76	2
MOL002670	Cavidine	35.64	0.81	28
MOL002714	Baicalein	33.52	0.21	37
MOL002776	Baicalin	40.12	0.75	2
MOL000358	Beta-sitosterol	36.91	0.75	38
MOL000449	Stigmasterol	43.83	0.76	31
MOL005030	Gondoic acid	30.7	0.2	2
MOL000519	Coniferin	31.11	0.32	22
MOL006936	10,13-eicosadienoic	39.99	0.2	2
MOL006937	12,13-epoxy-9-hydroxynonadeca-7,10-dienoic acid	42.15	0.24	0
MOL006957	(3S,6S)-3-(benzyl)-6-(4-hydroxybenzyl)piperazine-2,5-quinone	46.89	0.27	4
MOL003578	Cycloartenol	38.69	0.78	1
MOL006967	Beta-D-Ribofuranoside, xanthine-9	44.72	0.21	3

TCMSP, Traditional Chinese Medicine Systems Pharmacology Database and Analysis Platform.

drug, inserts were cultured in 5% CO_2 at 37 ℃ for 24 h. The non-transferred cells in the upper chamber were wiped off with a cotton swab and rinsed with phosphate-buffered saline (PBS), and the cells were fixed with methanol. After staining with 0.1% crystal violet, 5 fields were selected from each well and photographed under a light microscope, and the number of migrated cells in each group was counted.

Western blot analysis

For Western blot analysis, after cell culture medium was discarded, the culture was washed once or twice with PBS, the cell culture flask was placed on ice, the cells were scraped with a cell scraper, centrifugation was conducted at 1,000 g/min for 10 min, and the cells were collected. Radioimmunoprecipitation assay (RIPA) lysates were lysed for 30 min, proteins were quantified by bicinchoninic acid (BAC), and membranes were transferred overnight using SDS-PAGE (sodium dodecyl sulfate-polyacrylamide gel electrophoresis). Following this, 5% nonfat dry milk was blocked for 1 h at room temperature and incubated with the following primary antibodies: GAPDH (glyceraldehyde-3-phosphate dehydrogenase) antibody: (1:5,000; ab8245, Abcam, Abcam, USA), Akt: (1:500; ab8805, Abcam, USA), p-Akt: (1:750; ab38449, Abcam, USA), p-GSK-3β (1:10,000; ab75814, Abcam, USA), and GSK-3β (1:1,000; ab93926, Abcam, USA). After washing and soaking with TBST (tris-buffered saline with tween 20) ×3 for 10 min, the membrane was washed with secondary antibody incubation, and then electrochemiluminescence (ECL) chemiluminescence development was performed and images were collected for analysis.

Statistical analysis

A minimum of three biological replicates were performed for each experiment. Experimental data are presented as the mean ± standard deviation, and differences between groups were compared using a *t*-test and analyzed using GraphPad Prism 7.0 software (GraphPad Software, USA).

Results

Network pharmacological analysis

Common target genes of the main active compounds of RP and EC

A total of 116 chemical constituents of *P. ternata* were retrieved from TCMSP database, and 13 active compounds were obtained after screening using OB value ≥30% and DL ≥0.18. After prediction via the TCMSP online target platform, all targets were found except MOL006937, among which β-sitosterol (MOL000358) had the most target genes with 35 identified, followed by baicalein (MOL002714) with 31, and stigmasterol (MOL000449) with 28, and the above targets were 87 after de-weighting (*Table 1*; *Figure 1*; Table S1). Both β-sitosterol and stigmasterol are steroidal compounds with various

pharmacological effects such as anti-inflammation, anti-infection, maintaining cell membrane stability, inhibiting inflammation, preventing and treating atherosclerosis, and exerting anticancer effects (8,9). Baicalein, as a flavonoid, plays anti-inflammatory, antiangiogenic, and antimetastatic roles in cancer therapy (10). A total of 6,730 EC-related genes were screened. And using Venny 2.1, we crossed 87 "compound-target" genes with "esophageal cancer" target genes, and 68 consensus targets were obtained (*Figure 1*).

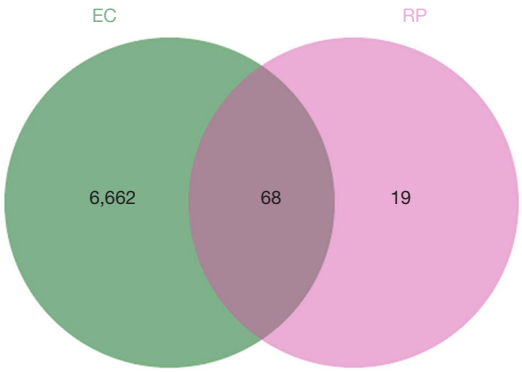

Figure 1 The Venn diagram of EC and RP. EC, esophageal cancer; RP, raw *Pinellia ternata*.

Construction and analysis of the compound-target gene-disease network model

The selected 12 candidate compounds and potential target genes were used to construct a network model using Cytoscape 3.6.1 software. Since the compound numbered MOL006937 has no target in the database, 99 nodes (12 candidate compounds and 87 targets) were included in the network model (*Figure 2A*). The analysis of 68 common targets showed that the genes responsible for the effects of RP and EC were Akt1, activator protein 1 (FOS/JUN), VEGF, matrix metalloproteinase-9 (MMP9), and hypoxia inducible factor-1 (HIF-1) (*Figure 2B*).

GO and KEGG analysis

GO and KEGG enrichment analysis of RP and EC cotarget genes were performed using the Metascape platform. Both GO and KEGG enrichment analyses filtered items based on P value <0.01) and enrichment ≥1.5. *Figure 3A* shows the top 20 significantly abundant categories for biological process (BP), cellular component (CC), and molecular function (MF) categories. In BP, target genes were found to be involved in G protein-coupled receptor signaling pathway, response to low oxygen levels, and cell communication; in CC, they are mainly involved

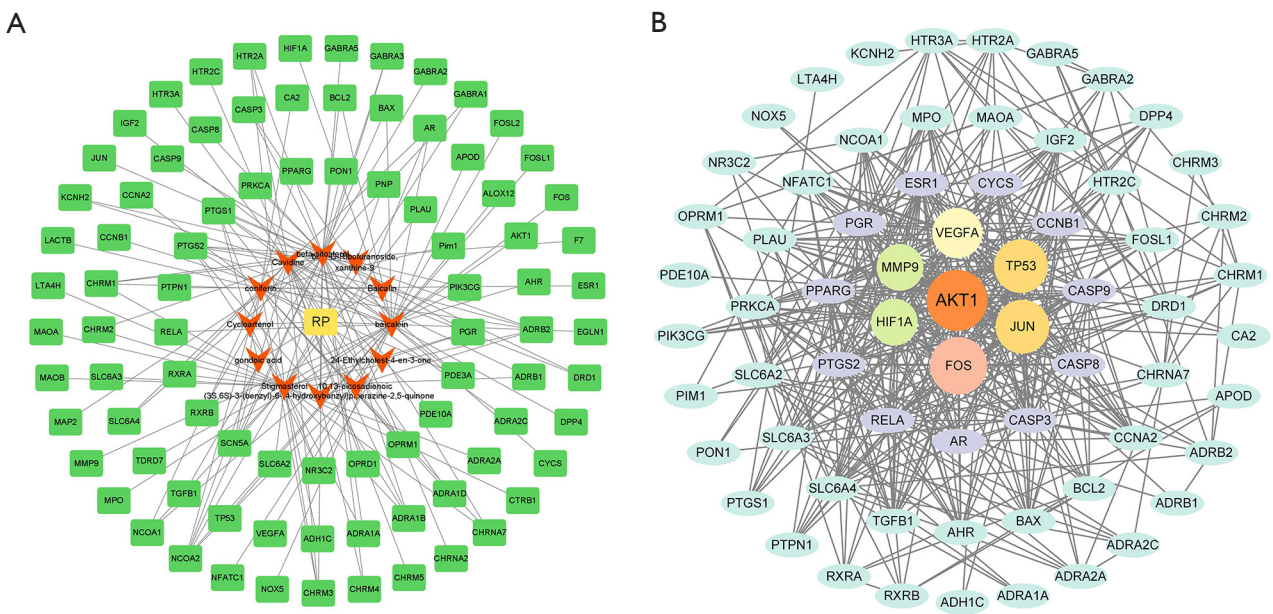

Figure 2 Construction and analysis of the network model of Compounds-target-Disease-pathway. (A) Potential target protein interaction network of the main active substances of *Pinellia ternate*. (B) Potential target protein interaction network of *Pinellia ternata* and the esophageal cancer target. RP, raw *Pinellia ternata*.

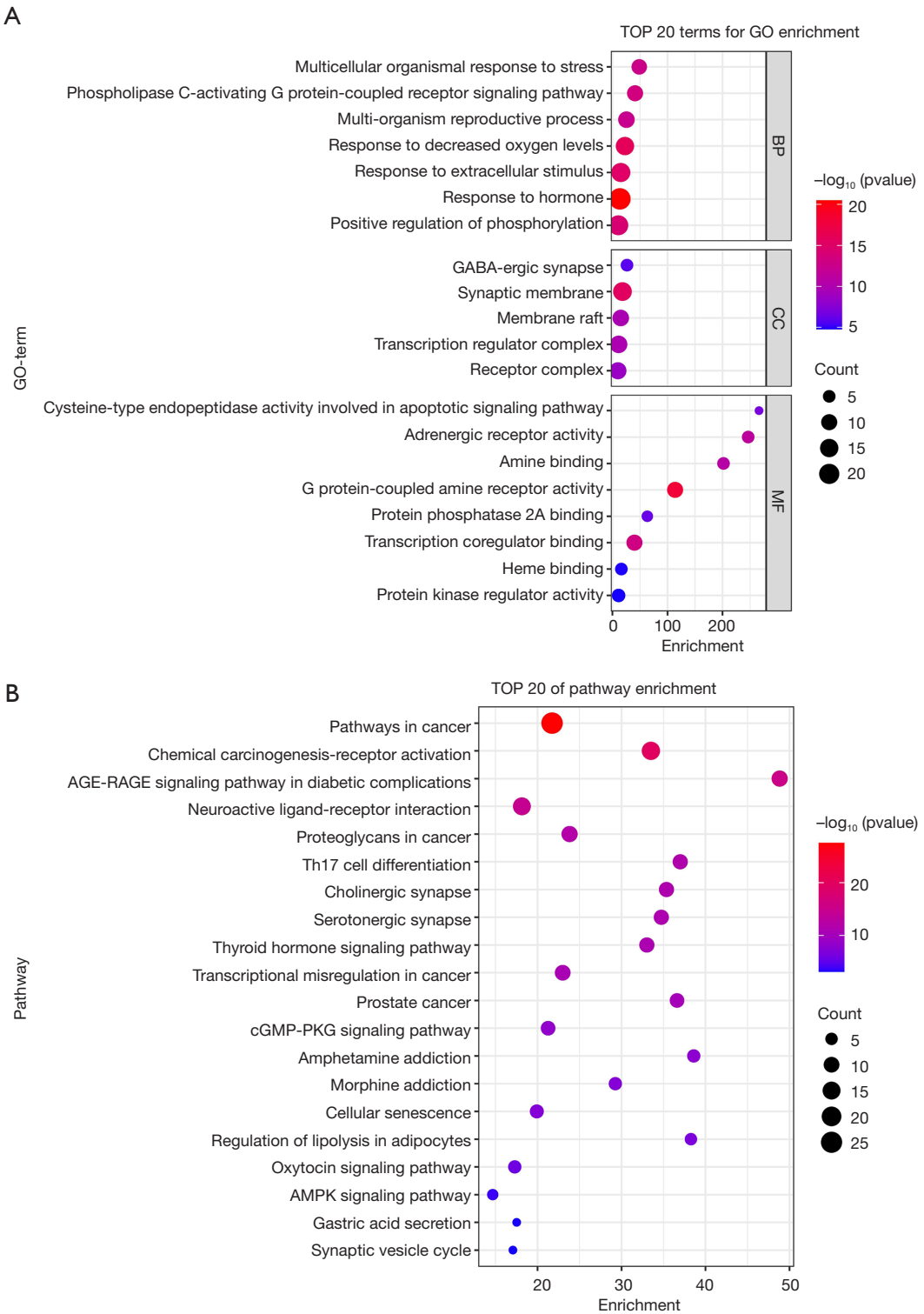

Figure 3 GO and KEGG analysis. (A) GO enrichment analysis of target genes. (B) KEGG pathway analysis of target genes. GO, gene ontology; BP, biological process; CC, cellular component; MF, molecular function; GABA, gamma-aminobutyric acid; AGE-RAGE, advanced glycation end product-receptor of AGE; cGMP-PKG, cyclic guanosine monophosphate-protein kinase G; AMPK, adenosine 5'-monophosphate (AMP)-activated protein kinase; KEGG, Kyoto Encyclopedia of Genes and Genomes.

in synapses, membranes, and transcriptional regulatory complexes; and in MF, they are involved in G protein-coupled amine receptor activity, transcriptional worker regulation, and apoptosis signaling pathway.

KEGG pathway enrichment analysis yielded a total of 144 significant pathways, 20 of which were mainly associated with advanced glycation end product-receptor of AGE (AGE-RAGE) signaling pathway, Th17 cell differentiation, thyroid hormone signaling pathway, transcriptional dysregulation of cancer, cyclic guanosine monophosphate-protein kinase G (cGMP-PKG) signaling pathway, cellular senescence, and adenosine 5'-monophosphate (AMP)-activated protein kinase (AMPK) signaling pathway (*Figure 3B*).

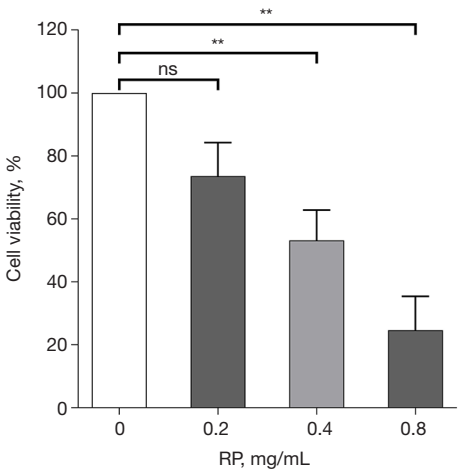

Figure 4 Effect of different concentrations of RP on the viability of Eca-109 cells. N=3 per group. ns, P>0.05; **, P<0.01. RP, raw *Pinellia ternate*.

Cell assay results

Cytotoxicity of RP on Eca-109 cells

The effect of RP on Eca-109 cell viability was tested using CCK-8 assay. Eca-109 cells were intervened with 0, 0.025, 0.05, 0.1, 0.2, 0.4, and 0.8 mg/mL of RP for 24 h. The results showed that RP significantly inhibited cell viability of Eca-109 cells at concentrations exceeding 0.2 mg/mL. Low concentrations of RP (<0.2 mg/mL) did not have a significant damaging effect on Eca-109 cells (0.025, 0.05, and 0.1 mg/mL were not significant and are not shown in *Figure 4*). Therefore, RP at a concentration of 0.2 mg/mL was selected for subsequent experiments.

RP inhibited TNF-α-induced migration of Eca-109 cells

The effects of TNF and RP treatment on the migration of Eca-109 cells were detected with scratch assays. The results showed that TNF-α induced the migration of Eca-109 cells. TNF-α significantly induced migration of ECA-109 cells compared as compared to control, and RP inhibited TNF-α-induced migration of Eca-109 cells (*Figure 5A*,*5B*).

RP inhibited TNF-α-induced phosphatidylinositol 3 kinase-protein kinase B (PI3K-Akt) signaling activation

Akt phosphorylation rose significantly after TNF-α treatment, and total Akt levels remained essentially unchanged in Eca-109 cells. This increased Akt phosphorylation peaked at 4 h of TNF-α intervention and then returned to basal levels (*Figure 6A*,*6B*). Glycogen

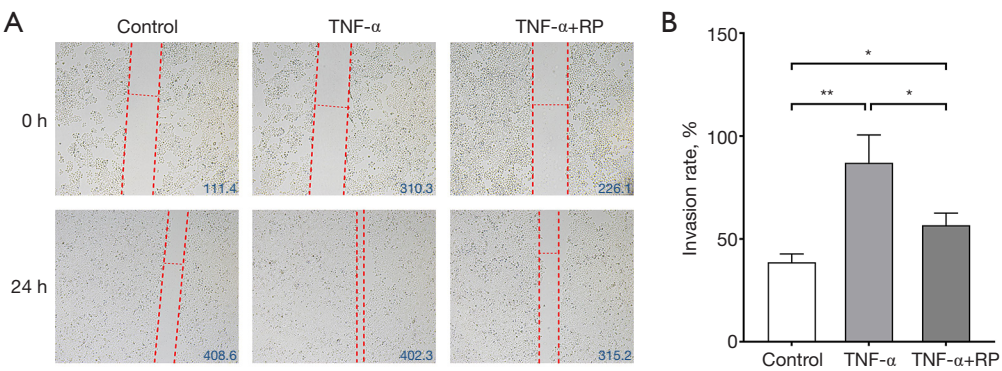

Figure 5 RP inhibited TNF-α-induced migration and invasion of Eca-109 cells. (A) The effect of RP on TNF-α-induced migration of Eca-109 cells was examined with the scratch test. Scale bar: 200 μm. (B) The mobility of Eca-109 cells was induced by TNF-α and RP. N=3 per group. *, P<0.05; **, P<0.01. TNF-α, tumor necrosis factor alpha; RP, raw *Pinellia ternate*.

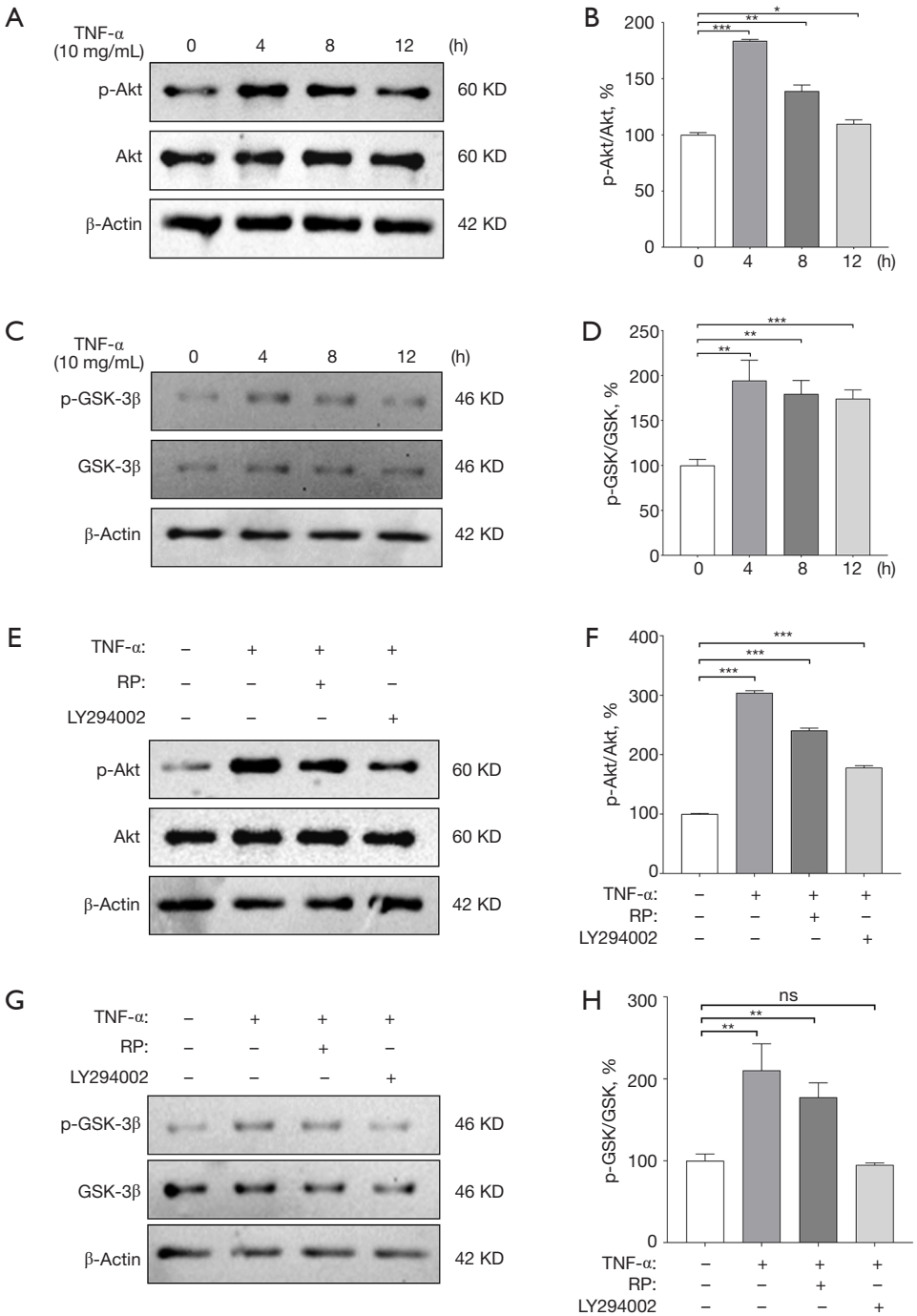

Figure 6 RP inhibited TNF-α-induced PI3K-Akt signaling pathway activation. (A) Western blot analysis of the effect of 10 mg/mL of TNF-α on the Akt phosphorylation levels at different times. (B) Akt phosphorylation ratio at different times. N=3 per group; *, P<0.05; **, P<0.01; ***, P<0.001. (C) Western blot analysis of the effect of 10 mg/mL of TNF-α on the GSK-3β phosphorylation levels at different times. (D) GSK-3β phosphorylation ratio at different times. N=3 per group; **, P<0.01; ***, P<0.001. (E) Western blot analysis of the Akt phosphorylation levels under different conditions. (F) Akt phosphorylation ratio under different conditions. N=3 per group; ***, P<0.001. (G) Western blot analysis of the GSK-3β phosphorylation levels under different conditions. (H) Phosphorylation ratio under different conditions. N=3 per group; ns, P>0.05; **, P<0.01. TNF-α, tumor necrosis factor alpha; RP, raw *Pinellia ternate*; PI3K-Akt, phosphatidylinositol 3 kinase-protein kinase B.

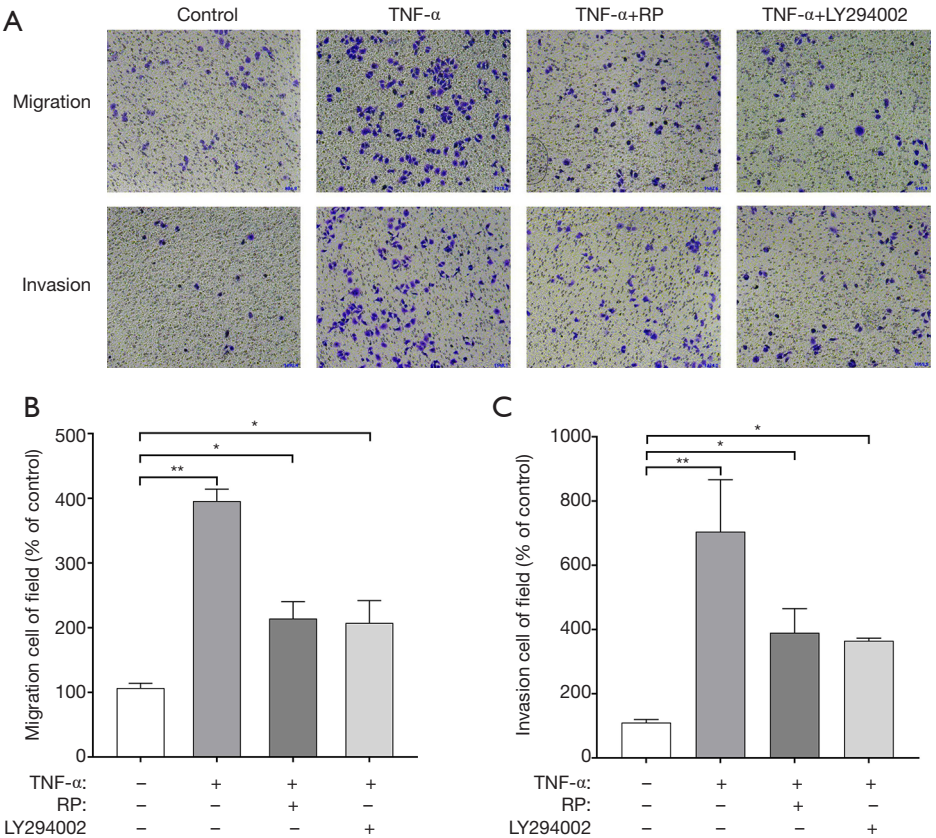

Figure 7 RP inhibited TNF-α-induced cell Eca-109 migration and invasion through PI3K-Akt signaling pathway. (A) The effects of RP and LY294002 on TNF-α-induced migration and invasion of Eca-109 cells were examined with Transwell assay. Scale bar: 200 μm. Adoption of crystal violet staining. (B) The migration rate of Eca-109 cells treated with TNF-α, RP, and LY294002. N=3 per group; *, P<0.05; **, P<0.01. (C) The invasion rate of Eca-109 cells treated with TNF-α, RP, and LY294002. N=3 per group; *, P<0.05; **, P<0.01. RP, raw *Pinellia ternate*; TNF-α, tumor necrosis factor alpha; PI3K-Akt, phosphatidylinositol 3 kinase-protein kinase B.

synthase kinase 3 (GSK-3β), as a major serine/threonine kinase, has already been shown to be aberrantly activated in EC (11). GSK-3β phosphorylation was found to peak at 4 h and gradually decrease after 4 h of TNF-α intervention (*Figure 6C,6D*). Therefore, TNF-α (10 ng/mL) was used to intervene the cells for 4 h to induce cell migration in the study. To further determine whether the inhibition of TNF-α-induced invasion by RP was mediated by the Akt signaling pathway, Eca-109 cells were treated with LY294002, a PI3K-Akt pathway inhibitor, for 4 h in the study, and the results showed that the degree of TNF-α-induced Akt phosphorylation and GSK-3β phosphorylation was reduced after RP intervention (*Figure 6E-6G*). LY294002 treatment of Eca-109 cells inhibited TNF-α-induced Akt phosphorylation and GSK-3β phosphorylation, which were the same as those of RP (*Figure 6E-6H*). This result suggests that PI3K-Akt signaling pathway may be involved in the anti-invasive effect of RP on Eca-109 cells.

RP inhibited TNF-α-induced cell Eca-109 migration and invasion through PI3K-Akt signaling pathway

Eca-109 cells were treated with TNF-α (10 ng/mL) and tested for cell migration with scratch assay. TNF-α significantly induced the migration and invasion of Eca-109 cells compared with control. TNF-α-induced migration and invasion of Eca-109 cells were reduced under RP treatment (*Figure* 7). To further determine whether the inhibition of TNF-α-induced migration and invasion by RP was mediated by Akt signaling, cells were treated with *P. ternata* and PI3K-Akt signaling pathway inhibitor LY294002, respectively. The results showed that RP significantly inhibited TNF-α-induced invasion of Eca-109 cells, which

was the same as the effect of inhibitor LY294002 (*Figure* 7). These results suggest that PI3K-Akt signaling pathway may be involved in the antimigration and anti-invasion activated of Eca-109 cells exerted by RP.

Discussion

EC is one of the most common and deadly cancers worldwide, and China is a country with a high incidence of this disease (12). Due to the limitations of gastroscopy and other diagnostic methods, EC is mostly diagnosed in the middle and advanced stages (13). Advanced EC has a low chance of surgery, and patients have a low 5-year survival rate and poor quality of life, with Western medical treatment consisting mostly of chemotherapy-based comprehensive treatment (14). TCM is currently an active research field aimed at identifying more effective cancer treatments. RP is commonly used in TCM for the clinical treatment of EC, and pharmacology has demonstrated that it has anti-inflammatory and antitumor effects (15). In this paper we investigated the active components of Shengbianxia and the common target genes of EC to determine its mechanism of action, which was verified by *in vitro* experiments.

In TCMSP database, OB and DL are generally utilized to screen the active ingredients of Chinese herbal medicines, OB is one of the most important pharmacokinetic characteristics of oral drugs, evaluating the efficiency of drug delivery to the systemic circulation, and DL predicts the drug similarity of the compounds and evaluates the possibility of drug formation, and molecules with high OB and DL parameters are likely to have good pharmacological activity (16). Therefore, based on the screening conditions, 13 active compounds were found in RP, of which only 12 existed as targets, and the number of targets after weight removal was 87. Sixty-nine targets shared by EC and RP were found in the construction of the "Component-Disease-Target" regulatory network map. Akt1, HIFIA and FOS were found to be the key targets of Biosynthia in EC (16,17). It has been shown that HIFIA can alleviate carotid atherosclerosis and airway allergic inflammation in rats through PI3K/Akt pathway, and HIFIA has not been investigated in EC, but it can antagonize PRC2 to promote tumorigenesis in breast and lung cancer (18). And JUN and FOS are associated with drug resistance in EC (19).

GO functional annotation and KEGG pathway enrichment results showed that the key targets screened mainly involved a series of biological response processes including drug immune response, oxidative stress response, and inflammatory response. The regulation of PI3K-Akt signaling pathway occupies a major position in the network diagram and can influence the activation status of various downstream effector molecules, which play a key role in inhibiting apoptosis and promoting proliferation in cells. Also the PI3K/AKT signaling pathway was significantly enriched in KEGG although not in the top 20. Moreover, the PI3K-Akt signaling pathway is closely related to the development of many human tumors, and the above results suggest the potential of RP in treating EC through the PI3K-Akt signaling pathway.

Akt is a critical component of signal transduction following PI3K activation, and a growing body of evidence suggests that PI3K-Akt signaling pathway is involved in TNF-α-induced morphological changes, migration, and invasion in various cell types (20,21). Activated Akt phosphorylated substrates can directly or indirectly affect downstream transcription factor activity (22,23). In this study, we demonstrated that RP was able to inhibit EC migration by *in vitro* migration assay, followed by WB assay which further showed that PI3K/Akt signaling pathway was activated in TNF-α-induced EC cell migration. Thus, PI3K-Akt is essential for the TNF-α-induced oncogenic transformation of cancer cells. In order to further verify that RP inhibited EC cell migration and invasion through PI3K-Akt, LY294002, a PI3K-Akt pathway inhibitor, was used to intervene Eca-109 cells in the study, and the results showed that LY294002 was able to significantly inhibit TNF-α-induced Eca-109 cell migration and invasion, with the effect being the same as that of RP. In summary, RP inhibits EC cell migration and invasion through the PI3K-Akt signaling pathway. Through network pharmacology, the interactive network of RP-active component-EC-target was constructed, and combined with modern molecular biology methods, it was proven that RP has the characteristics of multiple components, multiple targets, and multiple pathways for the treatment of EC. Moreover, for the first time, its mechanism of action was preliminarily explored through cell experiments, providing a basis for its in-depth development and utilization. However, this study only proved that RP can inhibit the migration and invasion of EC cells through PI3K-Akt pathway, and the additional pathways remain unexplored. Subsequently, the related pharmacodynamic mechanism will be systematically studied and verified in order to further elucidate the scientific connotation of RP in the treatment of EC and provide relevant instructive

experimental data.

Conclusions

In this study, we combined network pharmacology-based predictions and *in vitro* experiments to clarify the mechanism by which the target of RP and its major bioactive components effectively exert antinodal EC effects. We demonstrated that RP inhibits EC cell migration and invasion through the inhibition of the PI3K-Akt pathway. Based on this multidisciplinary strategy, this study provides a promising approach for using TCM to treat this disease.

Acknowledgments

The authors appreciate the great support from Dr. Xiongbin Lu (Indiana University School of Medicine, USA) in improving the quality of this paper.

Funding: This work was financially supported by the Special Subject of Scientific Research on Traditional Chinese Medicine in Henan Province (No. 2019ZY2036).

Footnote

Reporting Checklist: The authors have completed the MDAR reporting checklist. Available at https://jgo.amegroups.com/article/view/10.21037/jgo-23-684/rc

Data Sharing Statement: Available at https://jgo.amegroups.com/article/view/10.21037/jgo-23-684/dss

Peer Review File: Available at https://jgo.amegroups.com/article/view/10.21037/jgo-23-684/prf

Conflicts of Interest: All authors have completed the ICMJE uniform disclosure form (available at https://jgo.amegroups.com/article/view/10.21037/jgo-23-684/coif). The authors have no conflicts of interest to declare.

Ethical Statement: The authors are accountable for all aspects of the work in ensuring that questions related to the accuracy or integrity of any part of the work are appropriately investigated and resolved.

References

1. Huang FL, Yu SJ. Esophageal cancer: Risk factors, genetic association, and treatment. Asian J Surg 2018;41:210-5.
2. Bollschweiler E, Plum P, Mönig SP, et al. Current and future treatment options for esophageal cancer in the elderly. Expert Opin Pharmacother 2017;18:1001-10.
3. Kato H, Nakajima M. Treatments for esophageal cancer: a review. Gen Thorac Cardiovasc Surg 2013;61:330-5.
4. Dong X, Xu W, Shen J, et al. Research and application of raw Pinellia ternata in the treatment of malignant tumors. Journal of Traditional Chinese Medicine 2019;47:106-8.
5. Huang F, Gao J, Gong Q. Pharmacological Action and Toxicity of Pinellia ternata. Research and Development of Natural Products 2020;32:1773-81.
6. Wang Y, Wang Q. Progress in Chemical Composition, Pharmacological Action and Toxicity of Pinellia ternata. Chinese Pharmacy 2020;31:2676-82.
7. Shang L, Wang Y, Li J, et al. Mechanism of Sijunzi Decoction in the treatment of colorectal cancer based on network pharmacology and experimental validation. J Ethnopharmacol 2023;302:115876.
8. Khan Z, Nath N, Rauf A, et al. Multifunctional roles and pharmacological potential of β-sitosterol: Emerging evidence toward clinical applications. Chem Biol Interact 2022;365:110117.
9. Bakrim S, Benkhaira N, Bourais I, et al. Health Benefits and Pharmacological Properties of Stigmasterol. Antioxidants (Basel) 2022;11:1912.
10. Park YG, Choi J, Jung HK, et al. Baicalein inhibits tumor progression by inhibiting tumor cell growth and tumor angiogenesis. Oncol Rep 2017;38:3011-8.
11. Li MY, Fan LN, Han DH, et al. Ribosomal S6 protein kinase 4 promotes radioresistance in esophageal squamous cell carcinoma. J Clin Invest 2020;130:4301-19.
12. Wang M, Huo J, Kong J. Urban and rural difference analysis of malignant tumor deaths in China from 2002 to 2014. Practical Preventive Medicine 2018;25:1302-6.
13. Lewis S, Lukovic J. Neoadjuvant Therapy in Esophageal Cancer. Thorac Surg Clin 2022;32:447-56.
14. Chen J, Li H, Zhang Y, et al. Analysis of the characteristics of dominant population in the treatment of advanced

esophageal cancer with traditional Chinese medicine. Beijing Traditional Chinese Medicine 2021;40:880-2.
15. Zhang C. 16 Cases of malignant tumor treated with large dose of Pinellia ternata. Journal of Liaoning University of Traditional Chinese Medicine 2007;06:108-9.
16. Zhang W, Xue K, Gao Y, et al. Systems pharmacology dissection of action mechanisms of Dipsaci Radix for osteoporosis. Life Sci 2019;235:116820.
17. Lu HK, Huang Y, Liang XY, et al. Pinellia ternata attenuates carotid artery intimal hyperplasia and increases endothelial progenitor cell activity via the PI3K/Akt signalling pathway in wire-injured rats. Pharm Biol 2020;58:1184-91.
18. Tao X, Liu H, Xia J, et al. Processed product (Pinelliae Rhizoma Praeparatum) of Pinellia ternata (Thunb.) Breit. Alleviates the allergic airway inflammation of cold phlegm via regulation of PKC/EGFR/MAPK/PI3K-AKT signaling pathway. J Ethnopharmacol 2022;295:115449.
19. Mahara S, Lee PL, Feng M, et al. HIFI-α activation underlies a functional switch in the paradoxical role of Ezh2/PRC2 in breast cancer. Proc Natl Acad Sci U S A 2016;113:E3735-44.
20. Zhao Y, Luo A, Li S, et al. Inhibitor of Differentiation/DNA Binding 1 (ID1) Inhibits Etoposide-induced Apoptosis in a c-Jun/c-Fos-dependent Manner. J Biol Chem 2016;291:6831-42.
21. Jing ZT, Liu W, Xue CR, et al. AKT activator SC79 protects hepatocytes from TNF-α-mediated apoptosis and alleviates d-Gal/LPS-induced liver injury. Am J Physiol Gastrointest Liver Physiol 2019;316:G387-96.
22. Xu W, Yang Z, Lu N. A new role for the PI3K/Akt signaling pathway in the epithelial-mesenchymal transition. Cell Adh Migr 2015;9:317-24.
23. Ozes ON, Mayo LD, Gustin JA, et al. NF-kappaB activation by tumour necrosis factor requires the Akt serine-threonine kinase. Nature 1999;401:82-5.

Cite this article as: Liu Y, Bai Y, Zhang J, Silva-Filho R, Zhu Q, Lei Z. Utilizing network pharmacology and experimental validation to explore the potential molecular mechanisms of raw *Pinellia ternate* in treating esophageal cancer. J Gastrointest Oncol 2023;14(5):2006-2017. doi: 10.21037/jgo-23-684

Table S1 RP target gene summary

Mol ID	Molecule name	Target	Gene symbol
MOL001755	24-Ethylcholest-4-en-3-one	Progesterone receptor	*PGR*
		Mineralocorticoid receptor	*NR3C2*
MOL002670	Cavidine	Prostaglandin G/H synthase 1	*PTGS1*
		Muscarinic acetylcholine receptor M3	*CHRM3*
		Potassium voltage-gated channel subfamily H member 2	*KCNH2*
		Muscarinic acetylcholine receptor M1	*CHRM1*
		Beta-1 adrenergic receptor	*ADRB1*
		Sodium channel protein type 5 subunit alpha	*SCN5A*
		Coagulation factor Xa	
		Muscarinic acetylcholine receptor M5	*CHRM5*
		Prostaglandin G/H synthase 2	*PTGS2*
		5-hydroxytryptamine receptor 3A	*HTR3A*
		Alpha-2C adrenergic receptor	*ADRA2C*
		Muscarinic acetylcholine receptor M4	*CHRM4*
		Retinoic acid receptor RXR-alpha	*RXRA*
		Delta-type opioid receptor	*OPRD1*
		5-hydroxytryptamine 2A receptor	*HTR2A*
		5-hydroxytryptamine 2C receptor	*HTR2C*
		Alpha-1B adrenergic receptor	*ADRA1B*
		Beta-2 adrenergic receptor	*ADRB2*
		Alpha-1D adrenergic receptor	*ADRA1D*
		DNA topoisomerase II	
		Mu-type opioid receptor	*OPRM1*
		Heat shock protein HSP 90	
		Retinoic acid receptor RXR-beta	*RXRB*
		Calmodulin	
		Dopamine D1 receptor	*DRD1*
		Sodium-dependent serotonin transporter	*SLC6A4*
		Coagulation factor VII	*F7*
		cAMP and cAMP-inhibited cGMP 3',5'-cyclic phosphodiesterase 10A	*PDE10A*
MOL002714	Baicalein	Prostaglandin G/H synthase 1	*PTGS1*
		Androgen receptor	*AR*
		Prostaglandin G/H synthase 2	*PTGS2*
		Heat shock protein HSP 90	
		mRNA of PKA Catalytic Subunit C-alpha	
		Dipeptidyl peptidase IV	*DPP4*
		Phosphatidylinositol-4,5-bisphosphate 3-kinase catalytic subunit, gamma isoform	*PIK3CG*
		CGMP-inhibited 3',5'-cyclic phosphodiesterase A	*PDE3A*
		Trypsin-1	
		Nuclear receptor coactivator 2	*NCOA2*
		Nuclear receptor coactivator 1	*NCOA1*
		Calmodulin	
		Transcription factor p65	*RELA*
		RAC-alpha serine/threonine-protein kinase	*AKT1*
		Vascular endothelial growth factor A	*VEGFA*
		Apoptosis regulator Bcl-2	*BCL2*
		Proto-oncogene c-Fos	*FOS*
		Apoptosis regulator BAX	*BAX*
		Matrix metalloproteinase-9	*MMP9*
		Caspase-3	*CASP3*
		Cellular tumor antigen p53	*TP53*
		Hypoxia-inducible factor 1-alpha	*HIF1A*
		Fos-related antigen 1	*FOSL1*
		Fos-related antigen 2	*FOSL2*
		Cell division control protein 2 homolog	
		G2/mitotic-specific cyclin-B1	*CCNB1*
		Myeloperoxidase	*MPO*
		Aryl hydrocarbon receptor	*AHR*
		Insulin-like growth factor II	*IGF2*
		Cytochrome c	*CYCS*
		Arachidonate 12-lipoxygenase, 12S-type	*ALOX12*
		Nuclear factor of activated T-cells, cytoplasmic 1	*NFATC1*
		Tudor domain-containing protein 7	*TDRD7*
		Egl nine homolog 1	*EGLN1*
		NADPH oxidase 5	*NOX5*
		Fatty acid-binding protein, epidermal	
		Apolipoprotein D	*APOD*
MOL002776	Baicalin	Coagulation factor Xa	
		mRNA of Protein-tyrosine phosphatase, non-receptor type 1	*PTPN1*
MOL000358	Beta-sitosterol	Progesterone receptor	*PGR*
		Nuclear receptor coactivator 2	*NCOA2*
		Prostaglandin G/H synthase 1	*PTGS1*
		Prostaglandin G/H synthase 2	*PTGS2*
		Heat shock protein HSP 90	
		Phosphatidylinositol-4,5-bisphosphate 3-kinase catalytic subunit, gamma isoform	*PIK3CG*
		Potassium voltage-gated channel subfamily H member 2	*KCNH2*
		mRNA of PKA Catalytic Subunit C-alpha	
		Dopamine D1 receptor	*DRD1*
		Muscarinic acetylcholine receptor M3	
		Muscarinic acetylcholine receptor M1	
		Sodium channel protein type 5 subunit alpha	
		Gamma-aminobutyric-acid receptor alpha-2 subunit	*GABRA2*
		Muscarinic acetylcholine receptor M4	
		CGMP-inhibited 3',5'-cyclic phosphodiesterase A	*PDE3A*
		5-hydroxytryptamine 2A receptor	
		Gamma-aminobutyric-acid receptor alpha-5 subunit	*GABRA5*
		Alpha-1A adrenergic receptor	
		Gamma-aminobutyric-acid receptor alpha-3 subunit	*GABRA3*
		Muscarinic acetylcholine receptor M2	*CHRM2*
		Alpha-1B adrenergic receptor	*ADRA1B*
		Beta-2 adrenergic receptor	*ADRB2*
		Neuronal acetylcholine receptor subunit alpha-2	*CHRNA2*
		Sodium-dependent serotonin transporter	*SLC6A4*
		Mu-type opioid receptor	*OPRM1*
		Gamma-aminobutyric acid receptor subunit alpha-1	*GABRA1*
		Neuronal acetylcholine receptor protein, alpha-7 chain	*CHRNA7*
		Cytochrome P450-cam	
		Apoptosis regulator Bcl-2	*BCL2*
		Apoptosis regulator BAX	*BAX*
		Caspase-9	*CASP9*
		Transcription factor AP-1	*JUN*
		Caspase-3	*CASP3*
		Caspase-8	*CASP8*
		Protein kinase C alpha type	*PRKCA*
		Transforming growth factor beta-1	*TGFB1*
		Serum paraoxonase/arylesterase 1	*PON1*
		Microtubule-associated protein 2	*MAP2*

Table S1 (*continued*)

https://dx.doi.org/10.21037/jgo-23-684

Table S1 (*continued*)

Mol ID	Molecule name	Target	*Gene symbol*
MOL000449	Stigmasterol	Progesterone receptor	*PGR*
		Mineralocorticoid receptor	*NR3C2*
		Nuclear receptor coactivator 2	*NCOA2*
		Alcohol dehydrogenase 1C	*ADH1C*
		Ig gamma-1 chain C region	
		Retinoic acid receptor RXR-alpha	*RXRA*
		Nuclear receptor coactivator 1	*NCOA1*
		Prostaglandin G/H synthase 1	*PTGS1*
		Prostaglandin G/H synthase 2	*PTGS2*
		Alpha-2A adrenergic receptor	*ADRA2A*
		Sodium-dependent noradrenaline transporter	*SLC6A2*
		Sodium-dependent dopamine transporter	*SLC6A3*
		Beta-2 adrenergic receptor	*ADRB2*
		Aldose reductase	
		Urokinase-type plasminogen activator	*PLAU*
		Leukotriene A-4 hydrolase	*LTA4H*
		Amine oxidase [flavin-containing] B	*MAOB*
		Amine oxidase [flavin-containing] A	*MAOA*
		mRNA of PKA Catalytic Subunit C-alpha	
		Chymotrypsinogen B	*CTRB1*
		Muscarinic acetylcholine receptor M3	*CHRM3*
		Muscarinic acetylcholine receptor M1	*CHRM1*
		Beta-1 adrenergic receptor	*ADRB1*
		Sodium channel protein type 5 subunit alpha	*SCN5A*
		5-hydroxytryptamine 2A receptor	*HTR2A*
		Alpha-1A adrenergic receptor	*ADRA1A*
		Gamma-aminobutyric-acid receptor alpha-3 subunit	*GABRA3*
		Muscarinic acetylcholine receptor M2	*CHRM2*
		Alpha-1B adrenergic receptor	*ADRA1B*
		Gamma-aminobutyric acid receptor subunit alpha-1	*GABRA1*
		Neuronal acetylcholine receptor protein, alpha-7 chain	*CHRNA7*
MOL005030	Gondoic acid	Prostaglandin G/H synthase 1	*PTGS1*
		Nuclear receptor coactivator 2	*NCOA2*
MOL000519	Coniferin	Muscarinic acetylcholine receptor M3	*CHRM3*
		Muscarinic acetylcholine receptor M1	*CHRM1*
		Estrogen receptor	*ESR1*
		Androgen receptor	*AR*
		Sodium channel protein type 5 subunit alpha	*SCN5A*
		Peroxisome proliferator activated receptor gamma	*PPARG*
		Prostaglandin G/H synthase 2	*PTGS2*
		Carbonic anhydrase II	*CA2*
		CGMP-inhibited 3',5'-cyclic phosphodiesterase A	*PDE3A*
		Alpha-1B adrenergic receptor	*ADRA1B*
		Beta-2 adrenergic receptor	*ADRB2*
		Alpha-1D adrenergic receptor	*ADRA1D*
		DNA topoisomerase II	
		Mu-type opioid receptor	*OPRM1*
		Cell division protein kinase 2	
		Beta-lactamase	*LACTB*
		Neuronal acetylcholine receptor protein, alpha-7 chain	*CHRNA7*
		Ig gamma-1 chain C region	
		Proto-oncogene serine/threonine-protein kinase Pim-1	*Pim1*
		Cyclin-A2	*CCNA2*
		Nuclear receptor coactivator 2	*NCOA2*
		Nuclear receptor coactivator 1	*NCOA1*
MOL006936	10,13-eicosadienoic	Prostaglandin G/H synthase 1	*PTGS1*
		Nuclear receptor coactivator 2	*NCOA2*
MOL006937	12,13-epoxy-9-hydroxynonadeca-7,10-dienoic acid		
MOL006957	(3S,6S)-3-(benzyl)-6-(4-hydroxybenzyl) piperazine-2,5-quinone	Androgen receptor	*AR*
		Prostaglandin G/H synthase 2	*PTGS2*
		Beta-2 adrenergic receptor	*ADRB2*
		Calmodulin	
MOL003578	Cycloartenol	Mineralocorticoid receptor	*NR3C2*
MOL006967	beta-D-Ribofuranoside, xanthine-9	Purine nucleoside phosphorylase	*PNP*
		Prostaglandin G/H synthase 2	*PTGS2*
		Purine nucleoside phosphorylase deoD-type	

This table 1 was created by the authors and the contents of the table were obtained from open access databases, with Mol ID, Molecule Name, and Target sourced from TCMSP, Gene symbol from UniProt database. RP, raw *Pinellia ternate*.

https://dx.doi.org/10.21037/jgo-23-684